

The Cosmological Unimportance of Low Surface Brightness Galaxies

C.C. Hayward, J.A. Irwin, J.N. Bregman

University of Michigan

Astronomy Department, 830 Dennison Building, University of Michigan, Ann Arbor, MI 48109-1042

`cchaywar@umich.edu, jairwin@umich.edu, jbregman@umich.edu`

ABSTRACT

We have searched for Type Ia supernovae (SNe Ia) in the local ($d \lesssim 60$ Mpc) Universe using *Northern Sky Variability Survey* (NSVS) data collected from the nightly optical surveys of the *Robotic Optical Transient Search Experiment* (ROTSE) Telescope. It was hoped that SNe Ia would provide a means to find previously-unknown low surface brightness (LSB) galaxies or displaced stars that would otherwise be very difficult to detect. The ROTSE data allowed us to survey 19,000 square degrees at declinations north of 0° , but we did not find a single SN Ia in a period of time covering roughly one year. Using known SNe Ia rates in bright galaxies, we set an upper limit on the optical luminosity density, \mathcal{L}_B , of LSBs in the local Universe. Using mean LSB baryonic and dynamical mass-to-light ratios, we find 95% upper limits for LSBs of $\mathcal{L}_B \leq 2.53 \times 10^8 L_{B,\odot} \text{ Mpc}^{-3}$, $\Omega_b \leq 0.0040$, and $\Omega_m \leq 0.036$. We conclude that LSBs and displaced stars are not a major constituent of matter in the local Universe.

Subject headings: galaxies: fundamental parameters — galaxies: luminosity function, mass function

1. INTRODUCTION

Low surface brightness (LSB) galaxies are usually defined as galaxies with B-band central surface brightness $\mu_{0,B} > 23.5 \text{ mag arcsec}^{-2}$. The lower central surface brightness of LSB galaxies makes them difficult to detect against the noise of the night sky. Therefore, they are systematically absent in many optical galactic surveys. In recent years, improved techniques to detect LSBs have been developed, and the bulk properties of LSBs are now

better understood (e.g., Bothun et al. 1997; Burkholder et al. 2001; Monnier Ragaigne et al. 2002). However, the space density of LSBs is still a matter of debate. It has been suggested that LSBs could comprise up to 50% of all galaxies (e.g., Bothun et al. 1997), and thus could represent a major repository of baryons in the Universe. If so, we may have to reconsider our notions of galaxy formation, as the standard Hubble sequence is solely based on high surface brightness (HSB) galaxies. Additionally, all previous galaxy surveys will be considered incomplete, and the luminosity function of the Universe and large-scale structure will be affected. Consequently, an important goal is to determine the contribution of LSB galaxies to the optical luminosity density (\mathcal{L}_B), Ω_b , and Ω_m of the local Universe.

If LSB galaxies are significant baryonic repositories in the local Universe, then Type Ia supernovae (SNe Ia) should be detected in LSB galaxies in addition to HSB galaxies. A SN Ia in a LSB galaxy can have an apparent magnitude much greater than the magnitude of the host galaxy. Therefore, such SNe Ia provide a way to find otherwise hard-to-detect LSB galaxies. Our strategy is to search for SNe Ia in nearby LSB galaxies by using data from a shallow, all-sky survey (rather than a pencil-beam survey) that images the sky on a nightly basis.

Note: Results contained here-in are based on the explicit assumption that the binary frequency in LSB galaxies is the same as in HSB galaxies.

2. DATA SET

We used data from the *Northern Sky Variability Survey* (NSVS), publicly available data (Wozniak et al. 2004) collected by the *Robotic Optical Transient Search Experiment*’s ROTSE-I telescope, an array of four cameras mounted on a common equatorial platform (Kehoe et al. 2001). The optics are four Cannon 200 mm focal length, f/1.8, telephoto lenses in FD mounts, which are combined with four Apogee Instruments AP-10 CCD cameras with Thomson 2048 x 2048 14 μm imagers. The pixel width of the CCDs is 14.4” (Akerlof et al. 2000).

Each lens has a 64 square degree field of view, so the array covers 256 square degrees. The ROTSE-I telescope can detect objects brighter than 15.5 mag (Kehoe et al. 2001). Images were taken with unfiltered CCD’s, but magnitude is calibrated to a modified B-band. Magnitude in the ROTSE band (Akerlof et al. 2000) is

$$m_{\text{ROTSE}} = m_V - \frac{m_B - m_V}{1.875}. \quad (1)$$

The main purpose of ROTSE is to search for an optical counterpart to gamma-ray bursters (GRBs). When a GRB is detected, the ROTSE telescopes quickly move and take an image at the position of the GRB. When not imaging GRBs, the ROTSE-I telescope was used to take two images in rapid succession of every visible field each night. These skypatrols cover the sky north of -38° declination twice nightly, but only the data north of 0° declination was suitable for our purposes. The data set we used spans a roughly one year period, from May 2000 to April 2001, though the length of time covered varies by field.

3. DATA ANALYSIS

The ROTSE-I data are useful for detection of Type Ia supernovae because of the nightly frequency of the skypatrols. We designed an algorithm to search for SNe Ia in the ROTSE skypatrols data by analyzing the shape of the light curve of each of the over 12 million objects in the data set. The algorithm can detect SNe Ia that peak at V magnitude 14.5 or brighter. Since SNe Ia have a standard absolute V magnitude of approximately -19.45 (Riess et al. 1999), the upper limit of 14.5 (minus absorption) defines the volume scanned for each field.

Our search is sensitive to Type Ia supernovae with LSB hosts or without hosts altogether. A SN Ia in an LSB galaxy will have a template light curve shape because the host galaxy's flux is at least a factor of 10 less than the flux of the supernova. If the galaxy contribution were brighter, the resulting light curve would significantly deviate from the SN Ia template curve and the supernova would not be detected by our algorithm. This is not the case for HSB galaxies, for which light from a supernova would be blended together with a comparable amount of galaxy light due to the large pixel size (14''.4) of the detector, unless the supernova were well-separated from the galaxy core. Using only fields of low absorption ($A_V \lesssim 0.5$), distances out to ~ 60 Mpc can be searched. Contamination from types of SNe other than Ia is not significant because the other types peak at a considerably dimmer magnitude than SNe Ia and therefore would not appear frequently in the volume probed.

3.1. The Automated Search Algorithm

In order to find supernovae in a field, we analyzed the light curves of each object in the field with an automatic filtering program. The development of this program was based on testing with Monte Carlo simulations. The filter was designed to maximize the number of potentially valid supernovae identified and minimize the number of false positives.

The program is composed of the following steps:

1. The image is trimmed to make the field square and to include only areas of the sky that were well-observed by ROTSE-I. This step ensures that each area of the sky is only covered once. Also, individual observations with magnitudes outside the calibrated range, 9.0 to 15.5 magnitude, are discarded.
2. Objects for which there are fewer than 10 observations are discarded because these light curves are too poorly sampled to determine whether or not they are supernovae.
3. We remove outliers from the light curves by comparing the light curves to actual SNe Ia light curves given in Branch (1998). This step eliminates data points that are most likely due to incorrect calibration.
4. Subsequently stricter criteria are applied to the objects' light curves: we discard observations that are > 0.3 magnitude dimmer than the previous observation if the observations are before the maximum and observations that are > 0.3 magnitude brighter than the previous observation if the observations are after maximum (i.e., we eliminate observations that drop too much when the light curve is increasing and rise too much when the light curve is decreasing). Additionally, the maximum and minimum must occur at least five days apart. These steps further refine the light curves by removing points that differ from the SN Ia light curve template.
5. Points that differ from the entire light curve's mean by more than 3σ are removed. This step should not affect SNe Ia light curves because these curves have relatively large σ .
6. If the modified light curve has less than 10 observations, the object is discarded.
7. A series of filters is applied to the modified light curve. These filters require the curve to vary with time in a manner consistent with typical SNe Ia light curves, taken from Branch (1998). Specifically, there must be at least one magnitude variation over the entire curve. We require all objects with light curves that peak below 12th magnitude to be visible for less than 150 days. All objects that peak between 12th and 9th magnitude must show at least 2 magnitudes variation. These filters eliminate most long-term variable stars.

3.2. Manual Examination of Results of Filtering Program

The filters described above yielded a set of possible SNe Ia for each field, which were subsequently examined by eye. The number of possible SNe Ia per field ranged from zero to hundreds, varying directly with Galactic latitude and inversely with the time coverage of

the field.

SIMBAD was used to determine if there are any known objects within the error box (15'') of the position of each possible SN Ia, in which case, the object is discarded. Otherwise, the Digitized Sky Survey (DSS) was used to obtain images of the sky near the possible SN Ia position. If there is an object visible in the images at the position of the possible SN Ia, it is unlikely that the object is an SN Ia in an LSB galaxy, since no supernovae that appeared during the ROTSE epoch would also appear during the epochs of the DSS images.

3.3. Testing the Search Algorithm

In order to test the efficacy of the filter, we generated a set of 10^3 synthetic SNe Ia light curves for each ROTSE field. The synthetic light curves have observations only for days that the actual field was observed, and the errors of a synthetic observation are randomly selected from the errors of actual observations with similar magnitude. The distribution of peak apparent magnitudes of the simulated SNe Ia is determined by assuming that all the simulated supernovae peak at absolute magnitude -19.45 and are distributed randomly throughout the field volume.

A SN Ia template light curve in the ROTSE band, created using V-band data from Hamuy et al. (1996), B-band data from Goldhaber et al. (2001), and Equation 1, is shown in Figure 1. Monte Carlo simulations were used to generate SNe Ia light curves from this template. An example of a SN Ia light curve (peak magnitude 13.59) generated by the Monte Carlo simulation program is shown in Figure 2.

We ran our filter program on each set of simulated SNe Ia, examined the results by eye, and recorded the percent identified as possible SNe Ia as the detection rate. For each field, the detection rate was multiplied by the total volume of space scanned and the total time the field was observed to obtain the effective detection region (i.e., the spatial volume and time period in which 100% of the SNe Ia peaking in the region would be detected). Dividing the sum of the effective detection regions for all the fields by the number of SNe Ia found yields an upper limit on the SNe Ia ($\text{SNe Mpc}^{-3} \text{ century}^{-1}$) rate for LSB galaxies.

The Monte Carlo simulations determined that the filtering program had a detection rate of 50-90% for most fields. The rate was nearly 100% for simulated SNe Ia peaking at 12th magnitude or higher but was significantly less for SNe Ia peaking below 12th magnitude. A plot of detection rate versus magnitude for a field with total detection rate of 66% is given in Figure 3.

The detection rate is intrinsically tied to the distribution of SNe Ia with respect to magnitude. An example of this distribution for 10^3 SNe Ia generated by the Monte Carlo simulation is given in Figure 4. In the simulation, all SNe Ia peak at an absolute magnitude of -19.45, so the apparent magnitude of a supernova immediately yields the distance to the supernova. The probability of detection of a SN Ia is directly proportional to volume scanned, so SNe Ia are preferentially observed at fainter magnitudes. Accordingly, the total detection rate is dominated by the lower detection rates for SNe Ia that peak below 12th magnitude.

3.4. Known SNe Ia in the Data Set

We tested the filtering program to determine if it could identify any previously known SNe Ia in the data set. The International Astronomical Union’s List of Supernovae was searched for all SNe Ia that meet the following requirements: The SN Ia was observable during the time period and area of sky for which we have data (roughly from May 2000 to April 2001 and north of 0° declination); it was bright enough (magnitude > 15.5) to be detected by ROTSE-I; and it was located further than ~ 30 arcseconds (2 pixels) from the host galaxy’s center. If the SN Ia was too close to the galaxy, the light curve will not resemble the SN Ia template, and our filtering program is not designed to detect such objects.

The only SN Ia found that met all three criteria was SN 2001V, which reached maximum light on March 5, 2001, with B magnitude 14.64 (Mandel et al. 2001). SN 2001V was located 64.6 arcseconds (~ 4.5 pixel widths) from its host galaxy, NGC 3987, a Type Sb spiral with B-band magnitude 14.4 (Vinkó et al. 2003). The position of SN 2001V was imaged frequently by ROTSE-I in late February and early March, so the SN Ia should be observed in the data, though only for a short time.

The filtering program did not identify a possible SN Ia at the position of SN 2001V. This is expected because the filter can only detect supernovae that peak at magnitude 14.5 or brighter. SN 2001V peaked at 14.64, so it is not possible to detect this supernova with the filtering program.

We checked to see if SN 2001V is in the original data set by searching for all objects observed by ROTSE-I near the position of SN 2001V. A few objects were found within an arcminute of SN 2001V, but they are not likely to be SN 2001V because they are a few magnitudes brighter than the supernova and show little variation. SN 2001V was brighter than magnitude 15.5 for only ~ 20 days (Vinkó et al. 2003), so the supernova may not be in the original data set. Thus the check for known SNe Ia is not possible, as no good candidates

exist.

4. CALCULATIONS AND RESULTS

The search algorithm yielded many objects for subsequent analysis, but none are confirmed SNe Ia. Many of the objects are known variable stars, and the others correspond to an object visible on the DSS. Therefore, we conclude that each candidate is a variable star.

The search program is effective because many known (and possibly many unknown) variable stars were found, and some of these objects have light curves that very closely resemble the SN Ia template. The Monte Carlo simulations indicate that over half of the simulated SN Ia peaking during observation of a field were detected. Since the filter is effective and detection rates were calculated, finding zero SNe Ia outside HSB galaxies is significant and can be used to place limits on the prevalence of LSB galaxies and displaced stars.

Upper limits on the number of SNe Ia in LSB galaxies in the data set were determined using Poisson statistics. Since we observed no SNe Ia, it was necessary to use single-sided statistics. There is a 16% chance of observing 0 SNe Ia in LSB galaxies if the expected value is 1.84 SNe Ia, so ≤ 1.84 SNe Ia is the single-sided 1σ confidence limit. Similarly, there is a 5% chance of observing 0 SNe Ia in LSB galaxies if the expected value is 3.00, so the 95% confidence limit is 3.00 SNe Ia.

For each field, the product of the detection rate (from the Monte Carlo simulations) and the total space and time searched yields an effective detection region. Summing this over all fields gives the total effective detection region (3.33×10^7 Mpc³ days).

We assume that SNe Ia occur at the same rate (number of SNe Ia per $L_{B,\odot}$) in LSBs as is observed in the local Universe. One objection to this assumption is that LSB galaxies may have binary fractions and/or star formation rates that differ significantly from those of HSB galaxies. However, binary formation is a local process (Tohline 2002), so, even though LSBs may have lower star formation rates than HSBs (Impey & Bothun 1997), the low stellar density of LSB galaxies will not affect the binary fraction. Though it was originally thought that LSBs are generally bluer than HSBs (Impey & Bothun 1997), the CCD survey of O’Neil et al. (1997) found LSBs with colors ranging from very blue to very red, suggesting that the previous lack of red LSBs was due to a selection effect. Thus the stellar population of LSBs is likely similar to that of HSBs, which also suggests that the SN Ia rates are similar. Furthermore, the HSB Type Ia supernova rate can be divided into a contribution from old progenitors and a contribution from young progenitors (Mannucci et al. 2005). The

old progenitor contribution is independent of the star formation rate and accounts for most of the SNe Ia in ellipticals, 50 percent in S0a/b, 20 percent in Sbc/d, and a few percent in irregulars. This contribution should also be present in LSBs. The young progenitor contribution is proportional to the SFR, and thus may be less important in LSBs. Therefore the SN Ia rate may be less in LSBs than HSBs, but not significantly less in ellipticals and early-type spirals. Though the assumption that the SN Ia rate in LSBs is the same as that in HSBs is reasonable, it is still an assumption, and it may be modified as supernovae in LSBs are studied further.

Cappellaro et al. (1999) determine that the SN Ia rate in HSB galaxies is 0.18 ± 0.05 SNe century $^{-1} 10^{-10} L_{B,\odot}$, so a lower limit on the SN Ia rate of ≥ 0.13 SNe century $^{-1} 10^{-10} L_{B,\odot}$ is adopted. Dividing the upper limits on the SN Ia rate per volume in LSB galaxies by the lower limit on the SN Ia rate per mass (Cappellaro et al. 1999) yields upper limits on the contribution of LSBs to the optical luminosity density of the local Universe.

We have calculated a mean LSB baryonic mass-to-light ratio of 2.20 (solar units) from the results of de Blok et al. (1996), Matthews et al. (2001), McGaugh & de Blok (1997), Monnier Ragaigne et al. (2003a,b), O’Neil, Bothun, & Schombert (2000), and Zavala et al. (2003). From the data of de Blok et al. (1996), McGaugh & de Blok (1998), and Zavala et al. (2003), we calculate a mean LSB dynamical mass-to-light ratio of 20.21. Note that the dynamical ratio is less certain than the baryonic ratio because the number of LSBs with calculated baryonic mass-to-light ratios is much greater than the number of LSBs with calculated dynamical mass-to-light ratios. We have used these typical mass-to-light ratios to set upper limits on the contribution of LSBs to Ω_b and Ω_m . The results of the calculations are listed in Table 1.

The optical luminosity density, \mathcal{L}_B , of HSB galaxies is $(1.35 \pm 0.14) \times 10^8 L_{B,\odot} \text{ Mpc}^{-3}$ (Fukugita & Peebles 2004).¹ The 1σ and 95% confidence upper limits on the optical luminosity density of LSBs are slightly above the HSB value, so LSBs and displaced stars contribute no more than an amount comparable to HSBs to the optical luminosity density of the local Universe.

We set upper limits on the contribution of LSBs to the mean Ω_b and Ω_m of the local Universe (Table 1). The upper limit on Ω_b for LSBs indicates that LSBs cannot increase the currently observed mean value of Ω_b in the Universe by more than 9 percent because $\Omega_b = 0.044 \pm 0.004$ (Bennett et al. 2003). Therefore, LSBs are not significant baryonic repositories in the local Universe. LSBs cannot increase the value of the mean Ω_m in the Universe by more than 13 percent because $\Omega_m = 0.27 \pm 0.04$ (Bennett et al. 2003). Thus

¹ $H_0 = 71 \text{ km s}^{-1} \text{ Mpc}^{-1}$ (Bennett et al. 2003) is used.

LSBs cannot account for a significant component of the total dark matter in the Universe.

5. DISCUSSION AND CONCLUSIONS

No supernovae were found in LSB galaxies (or outside known galaxies), and this result was used to set an upper limit on the optical luminosity density of LSBs and displaced stars in the local Universe. This also constrains the contribution of LSBs to Ω_b and Ω_m to be less than 9% and 13%, respectively. Therefore, LSBs do not account for a significant amount of missing baryons or dark matter.

Sprayberry et al. (1997) conducted an optical survey using the Advanced Plate Measuring (APM) system at Cambridge and calculated the luminosity function for LSB galaxies in the survey. They found that LSBs contribute approximately 30% to the field galaxy luminosity density. This agrees with our result that LSBs can contribute roughly no more than HSBs to the luminosity density.

Zwaan et al. (2001) conducted a blind strip survey of HI-selected galaxies in the 21-cm line. Since the survey was HI-selected, it avoided optical selection effects but only included gas-rich galaxies. They found no LSBs with central surface brightness $\mu_{0,B} > 24$ mag arcsec $^{-2}$. Zwaan et al. (2001) concluded that gas-rich LSBs (defined as $\mu_{0,B} > 23.0$ mag arcsec $^{-2}$) contribute no more than $5 \pm 2\%$ to the optical luminosity of the universe and no more than 11% to Ω_m .

Driver (1999) conducted a volume-limited sample of 47 galaxies from the Hubble Deep Field to find the local ($0.3 < z < 0.5$) bivariate brightness distribution. Driver (1999) found that LSBs ($21.7 < \mu_{0,B} < 24.55$) contribute $7 \pm 4\%$ to the optical luminosity density and $12 \pm 6\%$ to Ω_m . Note that our upper limit on Ω_m is in good agreement with both Zwaan et al. (2001) and Driver (1999).

Studies of intracluster starlight provide an indirect probe of the contribution of LSBs and displaced stars to the optical luminosity density of clusters. Feldmeier et al. (1998) conducted a survey for intracluster planetary nebulae (PN) in the Virgo Cluster. They detected PN by comparing sums of on-band images to sums of off-band images and picking point sources that were only visible in [O III]. Feldmeier et al. (1998) found that intracluster starlight accounts for between 22 and 61 percent of the optical luminosity density of the cluster. This result agrees with what has been found in the local Universe even though tidal disruption is more common in clusters than in the field.

Various authors have searched for LSBs in the Coma cluster (e.g., Andreon & Cuillandre

2002; Ulmer et al. 1996; Karachentsev et al. 1995). They have found numerous LSBs in the core of the cluster, but the LSBs are only a minor fraction of the luminosity density of the cluster. Bernstein et al. (1995) did a deep CCD integration of a region in the core of the Coma cluster and determined that LSBs contribute about 1/400 of the luminosity of the cluster.

It is encouraging that numerous different methods of studying the contributions of LSBs to the optical luminosity density and Ω_m yield consistent results, both for the local Universe and for clusters. These results all point to the conclusion that LSBs do not account for a significant amount of matter.

We would like to thank the ROTSE team, with special thanks to Tim McKay and Carl Akerlof, for allowing us access to their skypatrol data. ROTSE is a collaboration of Lawrence Livermore National Lab, Los Alamos National Lab, and the University of Michigan (www.umich.edu/~rotse). This research has made use of the SIMBAD database, operated at CDS, Strasbourg, France, the STScI Digitized Sky Survey (DSS) (http://archive.stsci.edu/cgi-bin/dss_form), the International Astronomical Union’s “List of Supernovae” (<http://cfa-www.harvard.edu/iau/lists/Supernovae.html>), operated by the Central Bureau for Astronomical Telegrams (CBAT), and the NASA/IPAC Extragalactic Database (NED), which is operated by the Jet Propulsion Laboratory, California Institute of Technology, under contract with the National Aeronautics and Space Administration.

REFERENCES

Akerlof, C., et al., 2000, AJ, 119, 1901

Andreon, S., & Cuillandre, J. -C., 2002, ApJ, 569, 144

Bennett, C. L., et al., 2003, ApJS, 148, 1

Bernstein, G. M., Nichol, R. C., Tyson, J. A., Ulmer, M. P., Wittman, D., 1995, AJ, 110, 1507

Bothun, G. D., Impey, C. D., & McGaugh, S. S., 1997, PASP, 109, 745

Branch, D., 1998, ARA&A, 36, 17

Burkholder, V., Impey, C. D., & Sprayberry, D., 2001, AJ, 122, 2318

Cappellaro, E., Evans, R., & Turatto, M., 1999, A&A, 351, 459

de Blok, W. J. G., McGaugh, S. S., & van der Hulst, J. M., 1996, MNRAS, 283, 18

Driver, S. P., 1999, ApJ, 526, L69

Feldmeier, J. J., Ciardullo, R., & Jacoby, G. H. 1998, ApJ, 503, 109

Fukugita, M., & Peebles, P.J.E., 2004, ApJ, 616, 643

Goldhaber, G., et al., 2001, ApJ, 558, 359

Hamuy, M., Phillips, M. M., Suntzeff, N. B., Schommer, R. A., Maza, J., Smith, R. C., Lira, P., & Aviles, R., 1996, AJ, 112, 2438

Impey, C., & Bothun, G., 1997, ARA&A, 35, 267

Karachentsev, I. D., Karachentseva, V. E., Richter, G. M., & Vennik, J. A., 1995, A&A, 296, 643

Kehoe, R., et al., 2001, ApJ, 554, L159

Mandel, K., Jha, S., Matheson, T., Challis, P., & Kirshner, R. P., 2001, American Astronomical Society Meeting 199, #47.04

Mannucci, F., Della Valle, M., Panagia, N., Cappellaro, E., Cresci, G., Maiolino, R., Petrosian, A., & Turatto, M., 2005, A&A, 433, 807

Matthews, L. D., van Driel, W., & Monnier-Ragaigne, D., 2001, A&A, 365, 1

McGaugh, S. S., & de Blok, W. J. G., 1997, ApJ, 481, 689

McGaugh, S. S., & de Blok, W. J. G., 1998, ApJ, 499, 41

Monnier Ragaigne, D., van Driel, W., Balkowski, C., Schneider, S. E., Jarrett, T. H., & O’Neil, K., 2002, Ap&SS, 281, 145

Monnier Ragaigne, D., van Driel, W., O’Neil, K., Schneider, S. E., Balkowski, C., & Jarrett, T. H., 2003a, A&A, 408, 67

Monnier Ragaigne, D., van Driel, W., Schneider, S. E., Balkowski, C., & Jarrett, T. H., 2003b, A&A, 408, 465

O’Neil, K., Bothun, G. D., & Schombert, J., 2000, AJ, 119, 136

O’Neil, K., Bothun, G. D., Schombert, J., Cornell, M. E., & Impey, C. D., 1997, AJ, 114, 2448

Riess, A. G., et al., 1999, AJ, 118, 2675

Sprayberry, D., Impey, C. D., Irwin, M. J. & Bothun, G. D., 1997, ApJ, 482, 104

Tohline, J. E., 2002, ARA&A, 40, 349

Ulmer, M. P., Bernstein, G. M., Martin, D. R., Nichol, R. C., Pendleton, J. L., & Tyson, J. A., 1996, AJ, 112, 2517

Vinkó, J., et al., 2003, A&A, 397, 115

Wozniak, P. R., et al., 2004, AJ, 127, 2436

Zavala, J., Avila-Reese, V., Hernández-Toledo, H., & Firmani, C., 2003, A&A, 412, 633

Zwaan, M. A., van der Hulst, J. M., de Blok, W. J. G., & McGaugh, S. S., 1995, MNRAS, 273, L35

Zwaan, M. A., Briggs, F. H., & Sprayberry, D., 2001, MNRAS, 327, 1249

Table 1. Upper Limits on LSB Galaxies

Parameter	1σ confidence	95% confidence	Observed values
SN Ia observed	≤ 1.84	≤ 3.00	
SN Ia rate (SN Mpc^{-3} century $^{-1}$)	$\leq 2.02 \times 10^{-3}$	$\leq 3.29 \times 10^{-3}$	
\mathcal{L}_B ($L_B \text{ Mpc}^{-3}$)	$\leq 1.55 \times 10^8$	$\leq 2.53 \times 10^8$	$(1.35 \pm 0.14) \times 10^8$ ^a
Ω_b	≤ 0.0025	≤ 0.0040	0.044 ± 0.004 ^b
Ω_m	≤ 0.022	≤ 0.036	0.27 ± 0.04 ^b

^aMean HSB value.

^bMean value for the Universe.

References. — The mean HSB \mathcal{L}_B value is from Fukugita & Peebles (2004). The Ω_b and Ω_m values are from WMAP (Bennett et al. 2003).

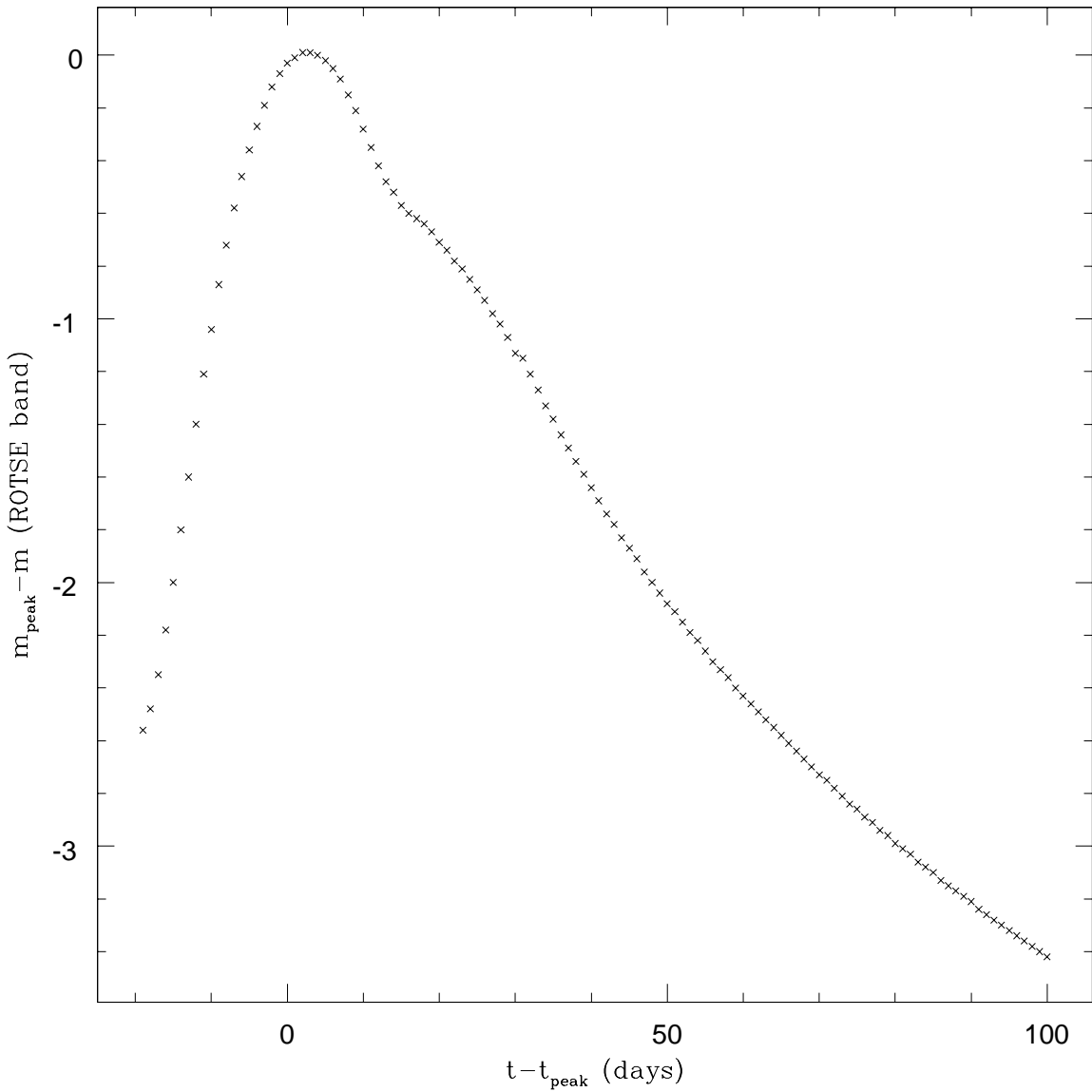


Fig. 1.— SN Ia light curve template in the ROTSE band, created from the B-band data of Goldhaber et al. (2001) and the V-band data of Hamuy et al. (1996).

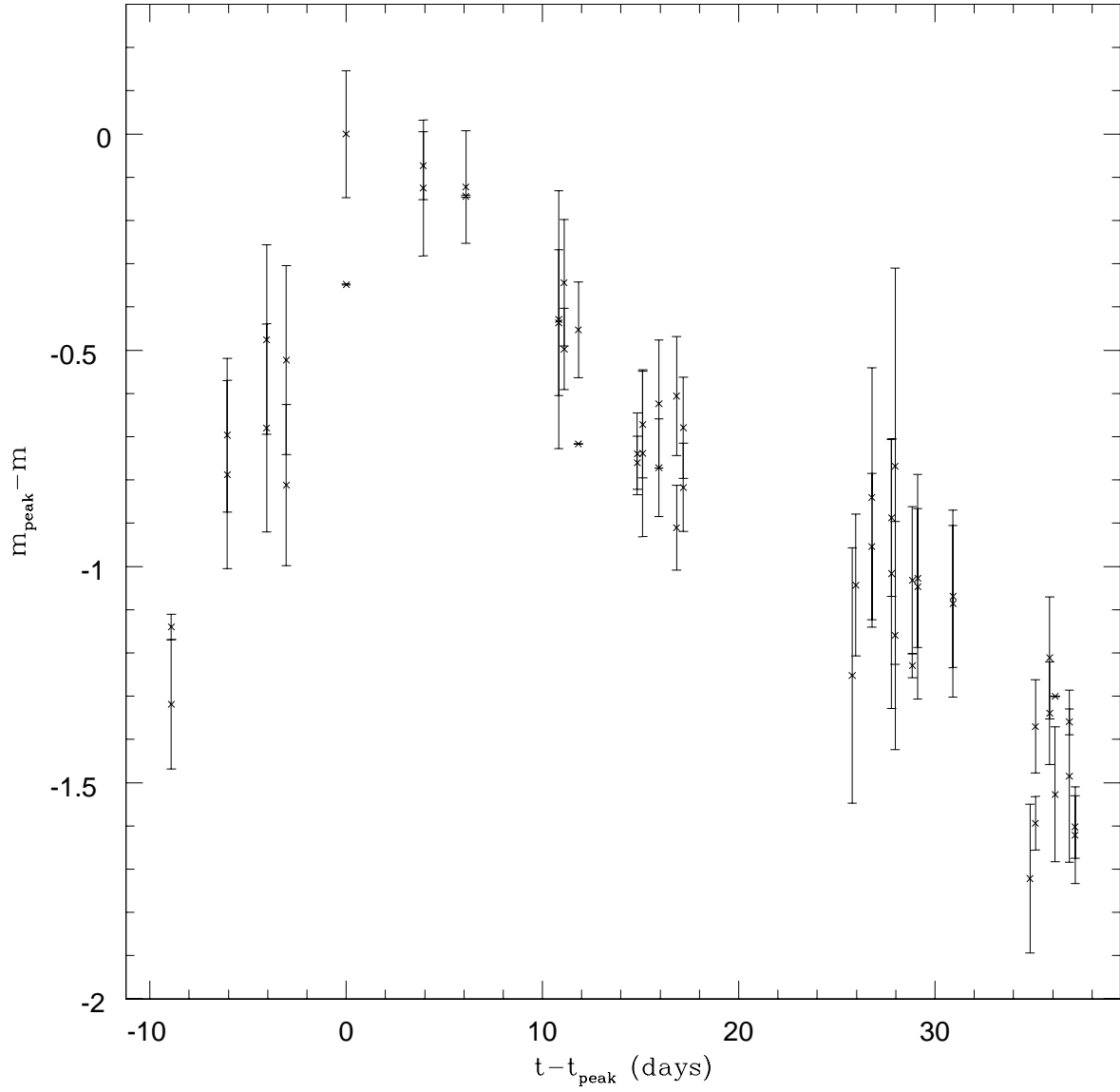


Fig. 2.— Light curve of a simulated SN Ia with peak magnitude 13.59 generated by our Monte Carlo program. Note that there are two separate observations for each day there is data.

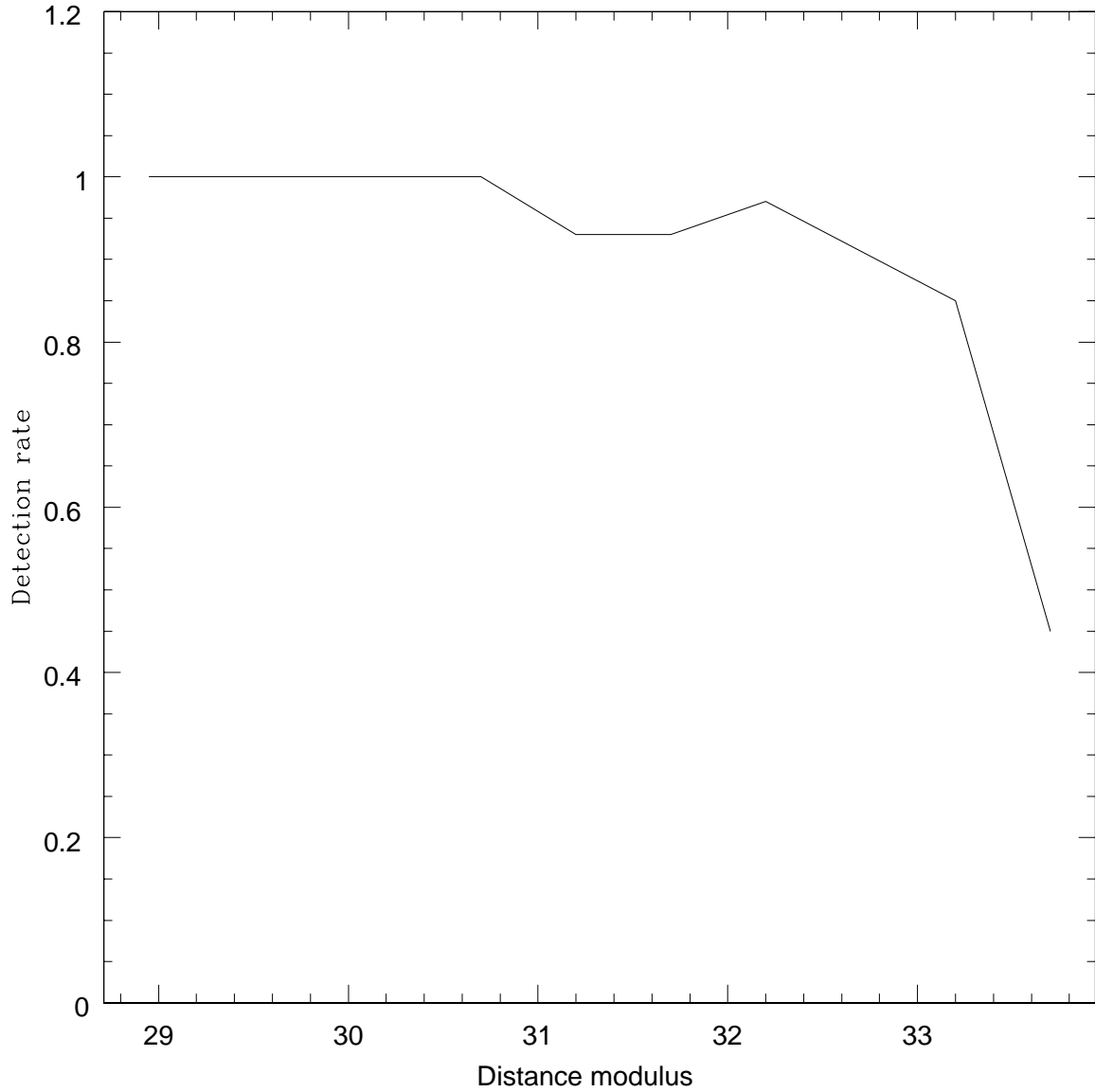


Fig. 3.— Detection rate of the filter vs. distance modulus, binned by 0.5 mag. The detection rate is almost 100% for SNe Ia observed at distance modulus less than 32, but the detection rate drops significantly for larger values of the distance modulus.

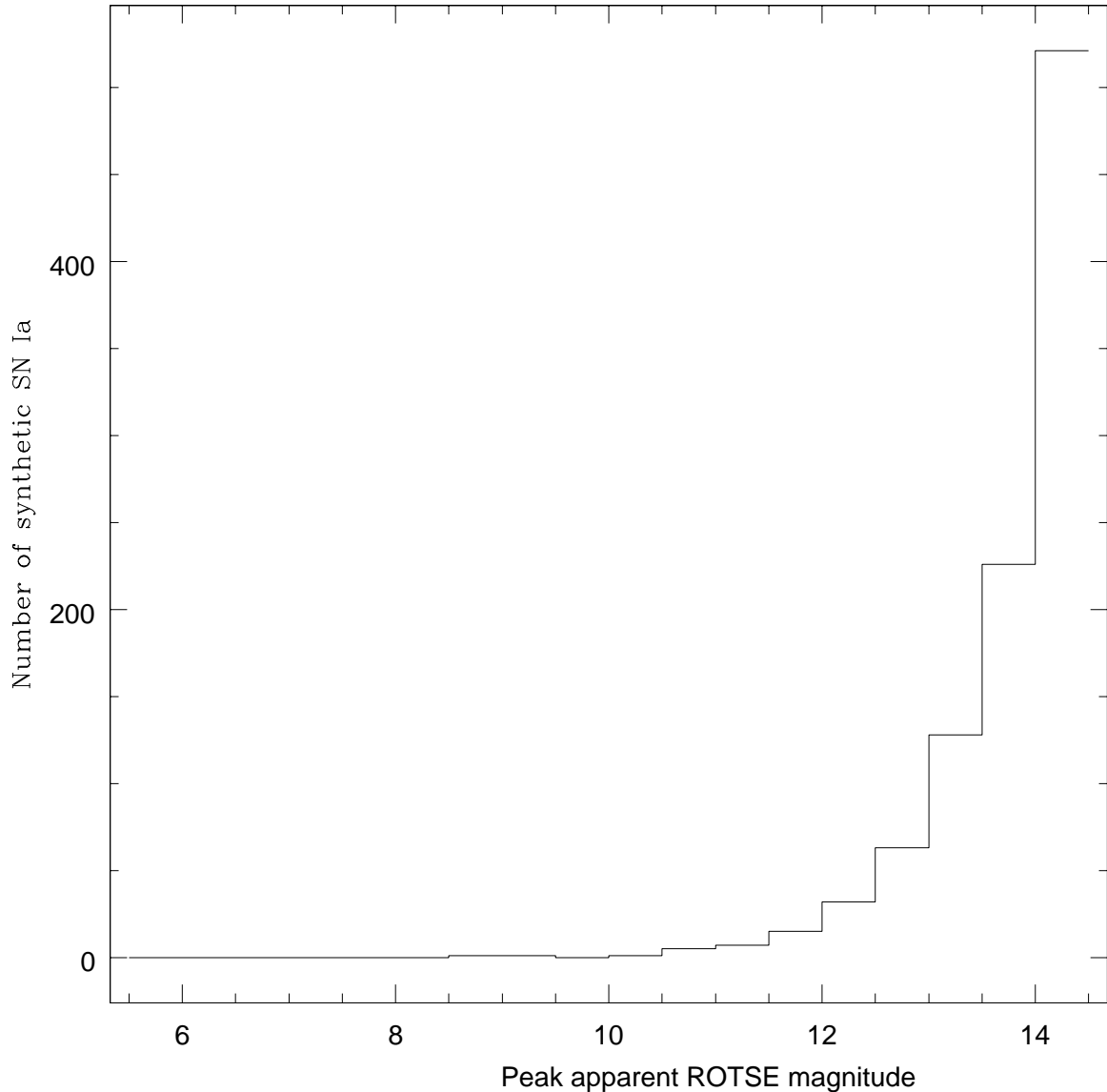


Fig. 4.— This example of the number of SN Ia generated by our Monte Carlo simulations as a function of magnitude illustrates how SN Ia are preferentially observed at fainter magnitudes.